Set of Performance Correlations for Reciprocating Compressor Covering Synthetic and Hydrocarbon Refrigerants

Owen DOUGHTY[1]*, Cordin ARPAGAUS[2], Stefan S. BERTSCH [2], Leon P. M. BRENDEL[2]

[1]Purdue, Mechanical Engineering,
West Lafayette, Indiana, USA

[2]OST – Eastern Switzerland University of Applied Sciences, Institute for Energy Systems,
9471 Buchs, Switzerland

*odoughty@purdue.edu

ABSTRACT

Accurate compressor performance prediction is a key tool in heat pump and refrigeration system modeling and design. Correlations applicable to a variety of refrigerant types are rare and would be valuable for multi-refrigerant screenings and mixture development. This work presents correlations for isentropic and volumetric efficiency and heat losses of reciprocating compressors for synthetic and hydrocarbon refrigerants and mixtures. A refrigerant-specific toggle term was included in the isentropic efficiency correlation to distinguish between refrigerant types. Equations were fitted to 365 experimental data points across two compressors, 7 pure fluids and 10 mixtures thereof, with pressure ratios ranging from 2 to 18, suction pressures from 50 to 750 kPa, isentropic efficiencies from 0.30 to 0.70, volumetric efficiencies from 0.35 to 0.90, and heat losses from 0.1 to 0.65 of the compressor power draw. The overall isentropic efficiency (referred to throughout the paper as simply "isentropic efficiency") correlation has three input parameters and predicts all data with an average deviation of 0.012. The volumetric efficiency correlation has only one input parameter and predicts all data with 0.022 average absolute error. The heat loss correlation has two input parameters and an average deviation of 0.034. All three correlations are valid over the entire experimental range for all fluid/compressor combinations tested.

Keywords: compressor performance, correlations, synthetic, hydrocarbons

1. INTRODUCTION

Refrigerant mixtures are a key optimization variable in high-temperature heat pumps. For realistic screening studies, the compressor as a key component must be accurately modeled for the range of considered refrigerants and mixtures. Many previous studies have attempted to characterize compressor performance (e.g., volumetric efficiency η_{vol}, overall isentropic efficiency η_{ois}, heat loss coefficient ζ_{co}) across operating conditions (e.g., suction and discharge pressure, superheat), but only a few evaluate a variety of different refrigerants on the same compressor.

Table 1 shows an overview of previously developed correlations in the open literature, most of which are fitted to specific refrigerants. Therefore, a screening study across refrigerants is not supported, indicating the need for an equation which is adaptable or simply agnostic to the fluid (but validated for several). Only two studies in Table 1 propose correlations for both synthetic and natural refrigerants. Roskosch et al. (2017) achieved this by providing refrigerant dependent coefficients which were validated also for fluids not included in the fitting procedure. Navarro-Peris et al. (2013) involved six different compressors, one with two different refrigerants tested. However, coefficients must be refitted for each refrigerant, making the correlation unsuitable for a multi-refrigerant screening.

Many approaches based on artificial neural networks, including Belman-Flores et al. (2015), Penz et al. (2012), Sanaye et al. (2011), and Yu et al. (2007), have achieved lower error for specific conditions (one compressor and one refrigerant). Still, the model's complexity and specificity make them unsuitable for this application.

The present study builds on Brendel et al. (2023) (with 200 data points) but is now based on an enlarged experimental dataset of 365 data points across two compressors, 7 pure fluids and 10 mixtures. Therefore, the correlations can now cover synthetic and hydrocarbon refrigerants.

Table 1: Previous correlations and their performance metrics published in the literature.

Literature reference	**η_{ois} error (relative)**	**η_{vol} error (relative)**	**Data points**	**Number of compressors**	**Number of fluids***	**η_{ois} inputs, coefficients**	**η_{vol} inputs, coefficients**	**Notes**
Navarro et al. (2007a)	Max 5%	Max 5%	85	4 reciprocating	1 refrigerant	10, -	-	
Navarro et al. (2007b)	Max 5%	Max 5%	-	4 reciprocating	1 synthetic 1 natural	3, -	-	Refit for each refrigerant
Navarro-Peris et al. (2013)	Max 5%	Max approx. 7%	100	1 scroll 5 reciprocating	1 synthetic 1 natural	3, 8	5, -	Builds on Pierre's correlations (Pierre, 1982)
Roskosch et al. (2017)	Avg 3% Max 6%	Avg 2.3% Max 6%	63	1 reciprocating	2 synthetic 4 natural	8, 4	8, 4	
Lumpkin et al. (2018)	Max 0.2%	Max 0.1%	43	1 reciprocating	1 synthetic	2, 10	-	Explored injection types, ζ_{co} correlation with 11% error
Brendel et al. (2023)	Avg 3.0% Max 21%	Avg 3.0% Max 14%	200	1 reciprocating	29 synthetic	2, 6	1, 2	Expanded for this study

2. AVAILABLE EXPERIMENTAL DATA

2.1 Experimental Test Bench

Figure 1 illustrates the schematic of the laboratory high-temperature heat pump used to generate three distinct datasets. A mass flow meter was installed in the liquid line, and an oil separator was directly downstream of the compressor. Thermocouples and pressure transducers were installed close to the compressor ports in insulated connecting pipes, but the compressor itself was not insulated. The compressor suction and discharge pressures were controlled by changing the heat sink and source temperature. The superheat was controlled using the expansion valve. The internal heat exchanger (IHX) was deactivated for all tests using a three-way valve. More detailed descriptions of the test setup can be found in Brendel et al. (2023) and Arpagaus et al. (2018).

Tests were conducted with two reciprocating compressors, called compressors A and B in the following. The compressors had similar outer dimensions and swept volumes of 0.158 and 0.153 liters, respectively. Tests with synthetic refrigerants were conducted with the polyester oil Reniso Triton SE 170, while tests with hydrocarbon refrigerant were performed with the polyalkylene glycol oil Reniso LPG 150. More information can be found in Fuchs (2023a) and Fuchs (2023b).

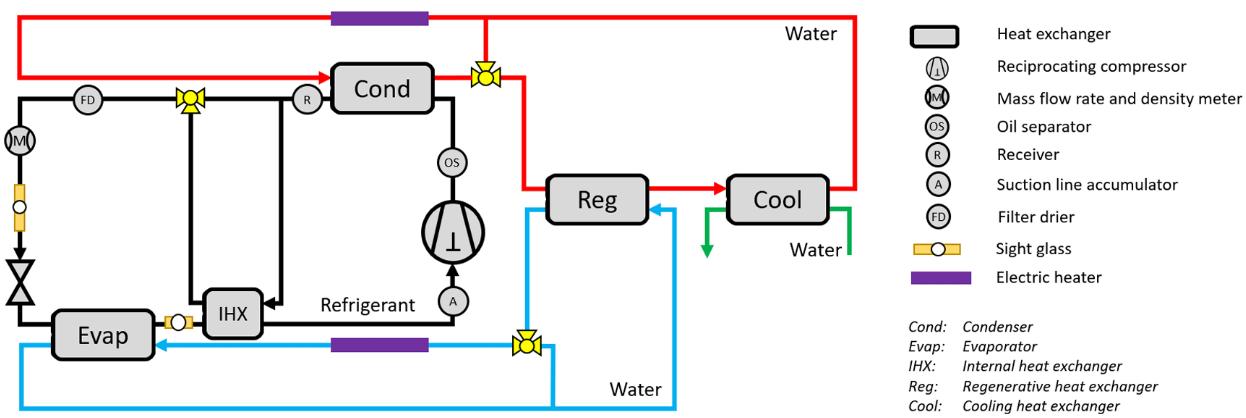

Figure 1: Schematic of experimental test setup.

2.2 Refrigerants

The refrigerants in this study can be classified into two families: hydrocarbon and synthetic. These refrigerant types perform differently, largely due to differing densities at equal pressures: the hydrocarbon refrigerants studied here have molecular masses in the range of 44 to 72 g/mol, less than half the values of synthetics at 102 to 164 g/mol (except R32, which was used at <20% mass concentration only).

2.3 Database

The data is categorized into three datasets.

- Dataset 1 is the dataset used in Brendel et al. (2023), consisting of synthetic refrigerants tested with compressor A.
- Dataset 2 consists of synthetic refrigerants tested with compressor B.
- Dataset 3 consists of hydrocarbon refrigerants tested on compressor B.

The datasets are shown in Table 2 with ranges of operating conditions for each relevant variable. From 368 total data points, three were removed: two for having suction pressures above 750 kPa and one for a pressure ratio (P_r) of 21, leaving the new maximum P_r at 18. Each steady-state data point was averaged over 10 minutes of operation. For 60 data points, all measurements were steady except the discharge temperature. These data points were excluded from the design and evaluation of the heat loss correlation but were still used for isentropic and volumetric efficiency correlations. Table 3 shows the specific refrigerants and mixtures tested in each dataset, with the numbers on the right indicating how many unique mixture ratios were tested.

Table 2: Evaluated datasets with ranges of important parameters.

Dataset	Number of data points	P_s [kPa]	P_r [-]	T_s [ºC]	T_{sh} [K]	d_s [kg/m³]	η_{ois} [-]	η_{vol} [-]	ζ_{co} [-]
1	256	41-745	2-18	3-104	5-52	3-35	0.30-0.68	0.37-0.91	0.09-0.62
2	48	156-675	3-10	49-86	16-52	8-27	0.57-0.66	0.63-0.84	0.13-0.36
3	61	143-701	2-12	19-87	10-53	3-13	0.33-0.68	0.47-0.89	0.11-0.29

Table 3: Tested refrigerants. The right column indicates the number of unique mass compositions tested.

Dataset 1	
R-1336mzz(Z)	
R-1233zd(E)	
R-1224yd(Z)	
R-1234yf	
R-1234yf /1336mzz(Z)	6
R-1234yf /1233zd(E)	3
R-32/1224yd(Z)	5
R-32/1224yd(Z)/1336mzz(Z)	1
R-32/1234yf/1224yd(Z)	8
R-32/1234yf/1336mzz(Z)	2
Dataset 2	
R-1224yd(Z)	
R-134a	
R-1234yf/1224yd(Z)	3
R-1234yf/1224yd(Z)/1336mzz(Z)	2
Dataset 3	
R-600	
R-290/600	11
R-290/601	8

3. CORRELATION FOR ISENTROPIC EFFICIENCY

3.1 Correlation Development

The overall isentropic efficiency η_{ois} is defined as the isentropic compression power for the measured mass flow rate $\dot{m}(h_{2s} - h_1)$ devided by the compressor power draw $\dot{W}$:

$$\eta_{ois} = \frac{\dot{m} \cdot (h_{2s} - h_1)}{\dot{W}} \tag{1}$$

The correlation developed by Brendel et al. (2023), Equation 2 below (hereafter referred to as the "London Correlation") served as the starting point for this investigation because it was able to predict efficiencies for a large number of different synthetic refrigerants and their mixtures.

$$\eta_{ois} = a_0 - \frac{0.6}{(P_r - a_1)^{a_2 \cdot P_s}} - a_3 \cdot P_r^{1.8} \tag{2}$$

P_r represents the pressure ratio and P_s the suction pressure. The coefficient a_0 sets an upper bound on the efficiency while the other terms subtract from this value. The second term defines the behavior for low pressure ratios, and the third term is for high pressure ratios. Higher suction pressures increase the efficiency as experimentally determined. This equation was originally fitted to Dataset 1 and was tested for Dataset 2 and 3 as they became available. It showed good results for Dataset 2, but significant errors occurred for Dataset 3 especially at high pressure ratios.

Thus, a "toggle term" R_x was introduced to account for the refrigerant type, taking on a different value for each refrigerant family (syn: synthetic, HC: hydrocarbon). This term replaced 1.8 in the London correlation to correct for the high-P_r outliers. This change causes steep drop-offs (see blue lines in Figure 2). Unfortunately, the trend is based on only a few data points. Another idea was using the suction density instead of the suction pressure in the denominator of the second term and moving R_x in place of London's a_2, but the maximum and average errors of the correlation could not be improved. Moreover, unlike suction density, suction pressure is a refrigerant-independent property making it easier to apply in some models.

The suction superheat T_{sh} was identified in Figure 3 as a relevant input not included in the London equation. Thus, the linear correction term $a_3 \cdot T_{sh}$ was added to the proposed correlation, reducing errors by about half. Because the a_1 term of the London equation is orders of magnitude below the value of P_r and increased the uncertainty of the coefficient solver, it was removed with no effect on the average and maximum errors. A static offset is visible for compressor B with synthetics, but it is small and not present for compressor B with hydrocarbons, so it was not addressed. Hence, the final form of the proposed correlation is:

$$\eta_{ois} = a_0 - \frac{a_1}{P_r^{a_4 \cdot P_s}} - a_2 \cdot P_r^{R_x} + a_3 \cdot T_{sh} \tag{3}$$

The values of the coefficients in this equation are shown in Table 4, along with the coefficients for later correlations. This equation was fitted for data with suction pressures in a range of 50 to 750 kPa, a pressure ratio range of 2 to 18 for synthetic and 2 to 15 for hydrocarbon refrigerants, and a suction superheat of 5 to 55 K. The trends of the correlation at 15 K superheat for fixed pressures of 150, 300, and 600 kPa are shown in Figure 2. An additional line (dashed) is plotted with 35 K superheat to show its effect. It should be noted that hydrocarbons in experimental data peak slightly higher than synthetics for each fixed-pressure curve, but the equation could not model this behavior without another refrigerant-specific term.

Table 4: Coefficients for proposed correlations.

	Overall isentropic efficiency							**Volumetric efficiency**		**Heat loss coefficient**	
Equation	Equation (3)							Equation (5)		Equation (7)	
Coefficient	a_0 [-]	a_1 [-]	a_2 [-]	a_3 [K^{-1}]	a_4 [kPa^{-1}]	R_{syn} [-]	R_{HC} [-]	b_0 [-]	b_1 [-]	c_0 [-]	c_1 [-]
Value	0.6462	0.5798	0.0012	0.0012	0.0077	1.712	2.047	0.0824	0.7277	0.1062	0.6463

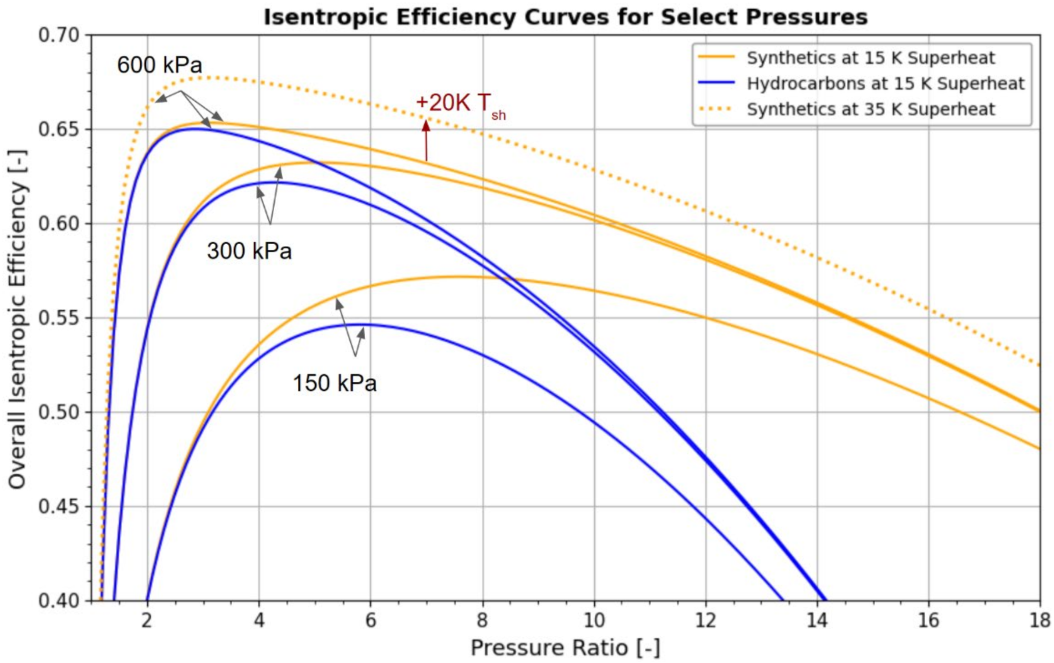

Figure 2: η_{ois} correlation vs. P_r at fixed pressures

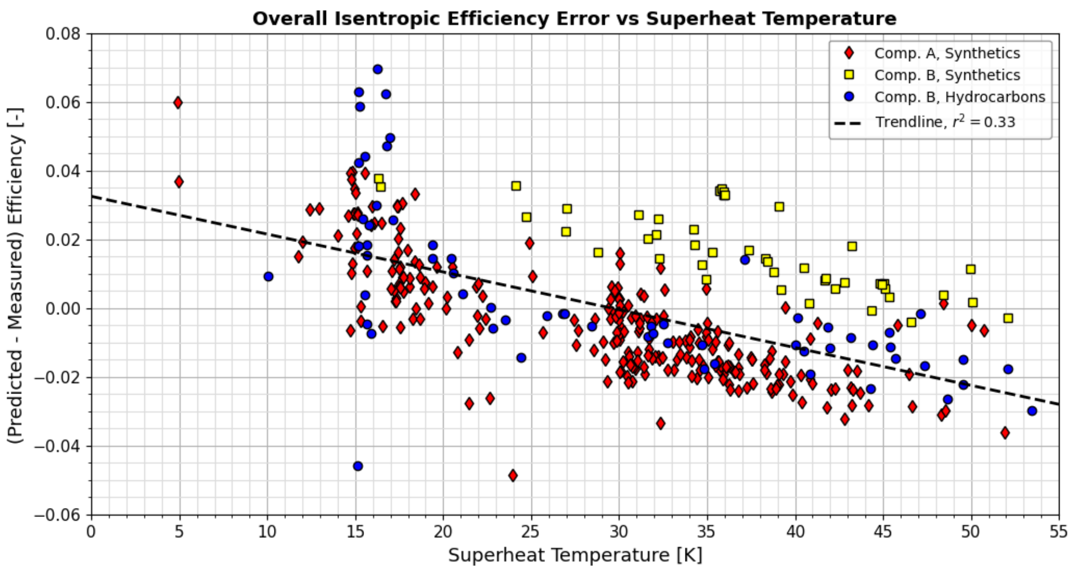

Figure 3: η_{ois} correlation error vs. suction superheat temperature

3.2 Correlation Performance

The performance of all investigated correlation equations was evaluated mainly by average and maximum deviation due to their intuitive meaning and relevance to system modeling applications. Figure 4 compares the performance of the London correlation (left) to the proposed correlation (right), with upper charts illustrating absolute error values as a function of the data point index number (chronological order of testing) and lower charts showing predicted efficiency as a function of measured efficiency with r^2 values included.

The London correlation predicts hydrocarbons particularly poorly. The proposed correlation corrects this by reducing the average error from 0.018 to 0.012 and the maximum error from 0.105 to 0.058. The first row of Table 5 contains the average and maximum absolute error values for the proposed isentropic efficiency correlation for all three datasets and each dataset.

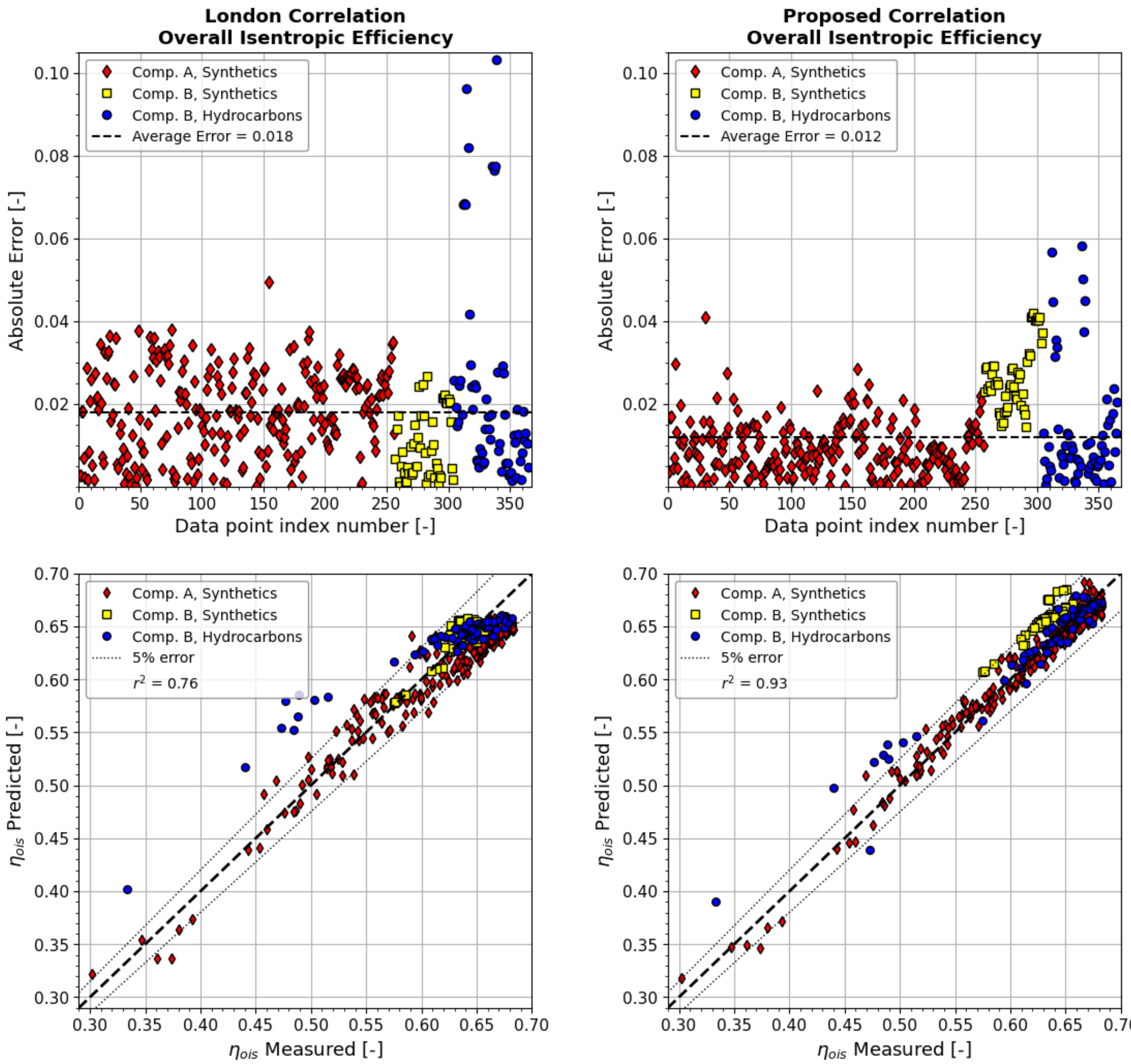

Figure 4: Absolute error of η_{ois} for the London correlation and the proposed correlation

Table 5: Absolute errors of the proposed correlations for all data and separate datasets. The first number in each cell indicates the average absolute error, and the number in parentheses shows the maximum error.

	All data	Dataset 1	Dataset 2	Dataset 3
Overall isentropic efficiency	0.012 (0.058)	0.009 (0.041)	0.027 (0.042)	0.013 (0.058)
Volumetric efficiency	0.022 (0.079)	0.012 (0.058)	0.025 (0.038)	0.013 (0.054)
Heat Loss	0.036 (0.238)	0.037 (0.238)	0.033 (0.075)	0.038 (0.081)

4. CORRELATION FOR VOLUMETRIC EFFICIENCY

The volumetric efficiency η_{vol} is defined as the actual mass flow rate over the theoretical one given the suction density ρ, the compressor frequency f and the swept volume of all cylinders combined V_{swept}:

$$\eta_{vol} = \frac{\dot{m}}{\rho \cdot f \cdot V_{swept}} \tag{4}$$

Despite being fitted only for Dataset 1, the London correlation for volumetric efficiency performs well for all datasets. There are some outliers but no clear dependencies. Refitting was deemed unnecessary as the decrease in the average error is small (0.001), and the maximum error increases by 0.008. The performance of the London volumetric efficiency equation (Equation 4) on the new datasets is graphed in Figure 5. It is repeated here for completeness, and the coefficients are presented in Table 4:

$$\eta_{vol} = 1 - b_0 \cdot (P_r - 1)^{b_1} \tag{5}$$

This equation was fitted for pressure ratios from 2 to 18, with overall and per-dataset average (and maximum) absolute errors detailed in Table 5.

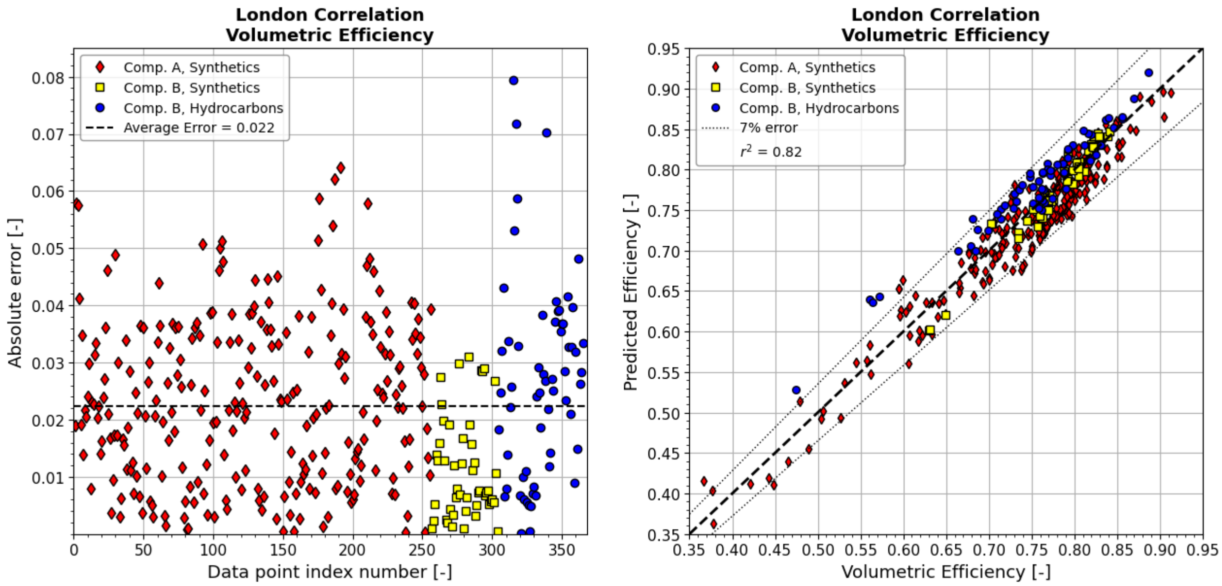

Figure 5: Volumetric efficiency η_{vol} performance for all datasets

5. CORRELATION FOR HEAT LOSS

5.1 Correlation Development

The heat loss factor ζ_{co} is defined as the heat losses $\dot{Q}_{lo}$ as calculated from an energy balance relative to the power draw of the compressor $\dot{W}$:

$$\zeta_{co} = \frac{\dot{Q}_{lo}}{\dot{W}} = \frac{\dot{W} - \dot{m} \cdot (h_2 - h_1)}{\dot{W}} \tag{6}$$

As mentioned in Section 2.3, some data points with unsteady discharge temperatures were not considered for this section of the investigation. Even after filtering, initial evaluations did not reveal strong correlations between any singular independent variable and heat loss, so more complex methods were employed. After filtering by suction temperature, some linear trends appeared relative to suction pressure.

Machine learning symbolic regression genetic algorithm gplearn (Stephens, 2016) was used to identify candidate equation forms and important variables. Many candidate equations were generated with varying complexity, performance, and physical sensibility. To narrow the field, the algorithm was tuned to minimize input parameters and total terms in the equations in addition to its default minimization of mean absolute error. Manually, equations with large growth/decay trends just outside the experimental range were pruned, as well as those with few major outliers.

Chiefly, this investigation confirmed that suction temperature and pressure were the best predictors of heat loss for this dataset, usually with pressure in the numerator and temperature in the denominator of a fraction. Exploration of error correction terms for equations with these two parameters suggested pressure ratio as a possible additional input. Still, no equation forms were developed with lower mean or maximum errors than the final equation. To cap output values at 1, the equation was constrained to the form 1 – (1/x), and after coefficients were rearranged, the final proposed equation took the following form:

$$\zeta_{co} = 1 - \frac{c_0}{1 + c_1\left(\frac{T_s}{P_s}\right)} \tag{7}$$

T_s is the suction temperature in °C, and the equation was fitted for values from 5 to 105 ˚C and suction pressures from 50 to 750 kPa. As with the previous correlations, its coefficient values are found in Table 4 and its error metrics in Table 5. In Figure 6, five curves of heat loss vs suction temperature are color-coded by suction pressure.

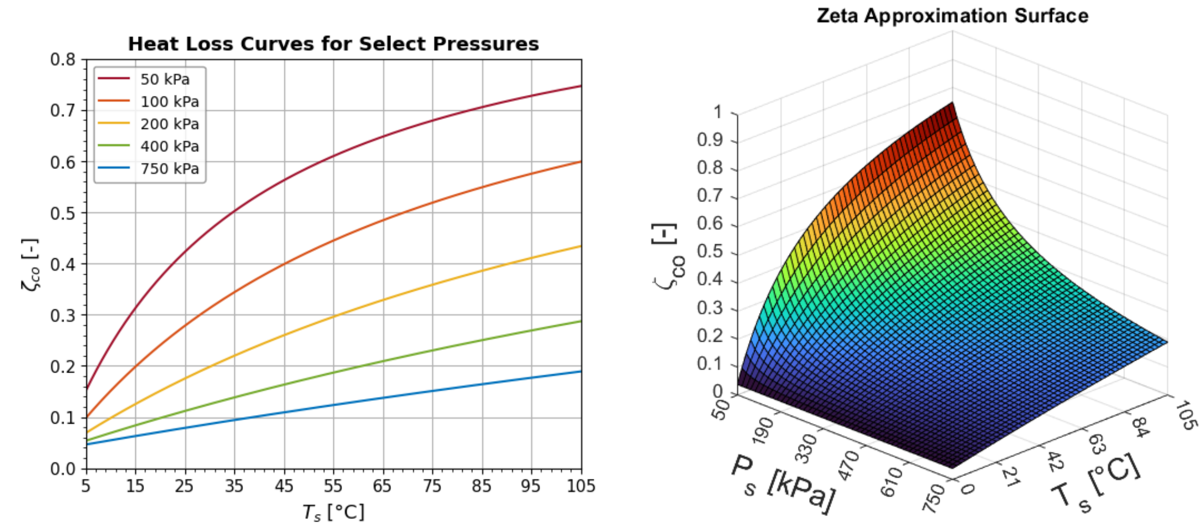

Figure 6: Heat loss ζ_{co} correlation representations in 2D (left) and 3D (right).

5.2 Correlation Performance

Figure 7 shows the absolute errors of the heat loss correlation vs. data point index number (left) and the measured value vs. predicted value (right). It shows that most points fall within ±20% despite the strongest outliers reaching a 53% maximum deviation.

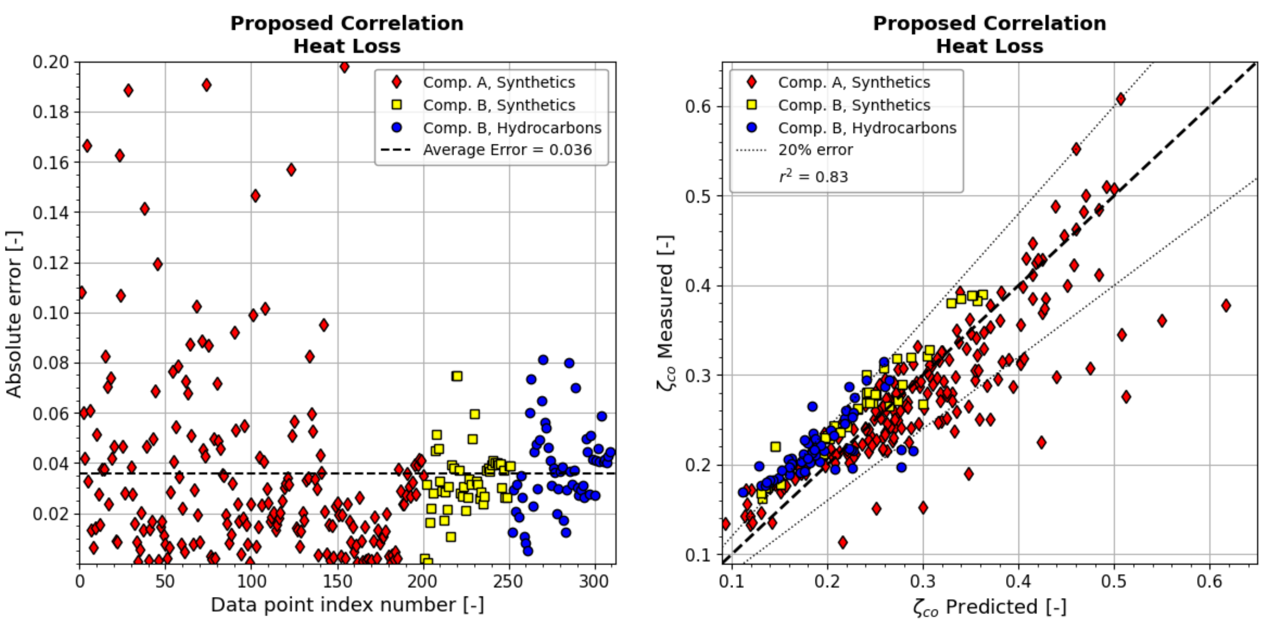

Figure 7: Absolute error of heat loss ζ_{co} for each dataset

6. CONCLUSIONS

This study compared and correlated data across two compressors and various refrigerants to correlate overall isentropic and volumetric efficiencies and the heat loss coefficient of a compressor with simple-to-use equations with the fewest possible input terms. The total number of data points for the final correlation equation fitting was 365, including 7 pure refrigerants and 49 total ratios of 10 different mixtures. The overall isentropic efficiency equation has 6 coefficients and 3 inputs (i.e., suction pressure, pressure ratio, and suction superheat). It was fitted with data considering suction pressures of 50 to 750 kPa, pressure ratios of 2 to 18 for synthetic and 2 to 15 for hydrocarbon refrigerants, and a suction superheat of 5 to 55 K. The equation requires a refrigerant "toggle term" for good results with synthetic and hydrocarbon (natural) refrigerants, predicting across all datasets with 0.012 average deviation and 0.058 maximum deviation. The volumetric efficiency correlation developed by Brendel et al. (2023) was verified for the additional refrigerants and compressor, showing a mean absolute error of 0.022 with a maximum of 0.079 for pressure ratios from 2 to 18. A heat loss correlation was developed with 2 input parameters (i.e., 5 to 105 ˚C suction temperature and 50 to 750 kPa suction pressure) and 2 coefficients, approximating the heat loss coefficient with 0.036 mean and 0.238 maximum errors. The refrigerant "toggle term" in the equation for the isentropic efficiency alludes to the possibility of building one general correlation for yet more refrigerants or compressor types.

NOMENCLATURE

P	Pressure	(kPa or unitless for P_r)
d	Density	(kg/m^3)
T	Temperature	(˚C)
a, b, c, R	Coefficients	(varying)
$\dot{W}$	Power draw	(kW)
$\dot{m}$	Mass flow rate	kg/s
V	Volume	(m^3)
η, ζ	Performance metrics	(-)

Subscript

r	ratio
s	suction
$2s$	statepoint assuming an isentropic process
d	discharge
sh	superheat
number	coefficient numbering

ACKNOWLEDGEMENTS

The authors gratefully acknowledge the financial support of the Swiss National Science Foundation and Innosuisse (Bridge Discovery project with grant number 203645). In addition, the financial support of the Swiss Federal Office of Energy (SFOE) as part of the SWEET (Swiss Energy research for the Energy Transition) project DeCarbCH (www.sweet-decarb.ch, project number SI/502260) is gratefully acknowledged.

REFERENCES

Arpagaus, C., Bless, F., Uhlmann, M., Büchel, E., & Frei, S. (2018). High temperature heat pump using HFO and HCFO refrigerants—System design, simulation, and first experimental results. Purdue Conferences, West Lafayette, IN, USA. https://docs.lib.purdue.edu/cgi/viewcontent.cgi?article=2874&context=iracc

Belman-Flores, J. M., Ledesma, S., Barroso-Maldonado, J. M., & Navarro-Esbrí, J. (2015). A comparison between the modeling of a reciprocating compressor using artificial neural network and physical model. *International Journal of Refrigeration*, *59*, 144–156. https://doi.org/10.1016/j.ijrefrig.2015.07.017

Brendel, L. P. M., Bernal, S. N., Roskosch, D., Arpagaus, C., & Bertsch, S. S. (2023). *Compressor performance for varying compositions of high-glide mixtures R1233zd(E)/R1234yf and R1336mzz(Z)/R1234yf.* 13th International Conference on Compressors and their Systems, London, England, ICCS 2023. Springer Proceedings in Energy. Springer, Cham. https://doi.org/10.1007/978-3-031-42663-6_60

Fuchs, 2023a. Reniso Triton SE170 [WWW Document]. Fuchs Lubr. Ger. GmbH. URL https://www.fuchs.com/de/en/product/product/148791-RENISO-TRITON-SE-170/

Fuchs, 2023b. Reniso Triton LPG150 [WWW Document]. Fuchs Lubr. Ger. GmbH. URL https://www.fuchs.com/de/en/product/product/151011-RENISO-LPG-150/

Lumpkin, D. R., Bahman, A. M., & Groll, E. A. (2018). Two-phase injected and vapor-injected compression: Experimental results and mapping correlation for a R-407C scroll compressor. *International Journal of Refrigeration*, *86*, 449–462. https://doi.org/10.1016/j.ijrefrig.2017.11.009

Navarro, E., Granryd, E., Urchueguía, J. F., & Corberán, J. M. (2007a). A phenomenological model for analyzing reciprocating compressors. *International Journal of Refrigeration*, *30*(7), 1254–1265. https://doi.org/10.1016/j.ijrefrig.2007.02.006

Navarro, E., Urchueguía, J. F., Corberán, J. M., & Granryd, E. (2007b). Performance analysis of a series of Hermetic reciprocating compressors working with R290 (propane) and R407C. *International Journal of Refrigeration*, *30*(7), 1244–1253. https://doi.org/10.1016/j.ijrefrig.2007.02.004

Navarro-Peris, E., Corberán, J. M., Falco, L., & Martínez-Galván, I. O. (2013). New non-dimensional performance parameters for the characterization of Refrigeration Compressors. *International Journal of Refrigeration*, *36*(7), 1951–1964. https://doi.org/10.1016/j.ijrefrig.2013.07.007

Penz, C. A., Flesch, C. A., Nassar, S. M., Flesch, R. C. C., & de Oliveira, M. A. (2012). Fuzzy–Bayesian Network for Refrigeration Compressor Performance Prediction and test time reduction. *Expert Systems with Applications*, *39*(4), 4268–4273. https://doi.org/10.1016/j.eswa.2011.09.10

Pierre, B.: Kylteknik, Allmän Kurs. Inst. Mekanisk Vä Rmeteori Och Kylteknik, KTH, Stockholm (1982) (in Swedish)

Roskosch, D., Venzik, V., & Atakan, B. (2017). Thermodynamic model for reciprocating compressors with the focus on fluid dependent efficiencies. *International Journal of Refrigeration*, *84*, 104–116. https://doi.org/10.1016/j.ijrefrig.2017.08.011

Sanaye, S., Dehghandokht, M., Mohammadbeigi, H., & Bahrami, S. (2011). Modeling of rotary vane compressor applying artificial neural network. *International Journal of Refrigeration*, *34*(3), 764–772. https://doi.org/10.1016/j.ijrefrig.2010.12.007

Stephens, T. (2016). *Welcome to gplearn's documentation!* gplearn 0.4.2 documentation. https://gplearn.readthedocs.io/en/stable/index.html

Yu, Y., Chen, L., Sun, F., & Wu, C. (2007). Neural-network based analysis and prediction of a compressor's characteristic performance map. *Applied Energy*, *84*(1), 48–55. https://doi.org/10.1016/j.apenergy.2006.04.005